ELSEVIER

Journal of Chromatography A, 969 (2002) 215–227

JOURNAL OF CHROMATOGRAPHY A

www.elsevier.com/locate/chroma

Surface energy characteristics of toner particles by automated inverse gas chromatography

L.H.G.J. Segeren[a,b], M.E.L. Wouters[b,c], M. Bos[d], J.W.A. van den Berg[a], G.J. Vancso[a,b,*]

[a]*Materials Science and Technology of Polymers, Faculty of Chemical Technology and MESA+ Research Institute, University of Twente, PO Box 217, 7500 AE Enschede, Netherlands*

[b]*Dutch Polymer Institute, PO Box 902, 5600 AX Eindhoven, Netherlands*

[c]*TNO Institute of Industrial Technology, PO Box 6235, 5600 HE, Eindhoven, Netherlands*

[d]*Chemical Analysis, Faculty of Chemical Technology and MESA+ Research Institute, University of Twente, PO Box 217, 7500 AE Enschede, Netherlands*

Abstract

Inverse gas chromatography (IGC) was applied to the surface energy study of surfaces of toner particles. The dispersive component of the surface energy was determined for three toner materials by infinite dilution IGC. The values obtained were comparable to the values obtained from contact angle experiments. Previous adhesion experiments by atomic force microscopy suggested that the toner is a hydrophilic material with multiple adsorption energy sites. Both aspects were at least qualitatively confirmed by finite concentration IGC. Several indications for surface heterogeneity were found: (i) the difference between the dispersive component of the surface energy determined by IGC and the unexpectedly low total surface energy as determined by droplet analysis, (ii) the strong tailing behavior of the peaks of the injected polar probes, (iii) the decrease of the net retention volume with increasing *n*-pentane concentration, and finally (iv) the broad energy site distribution function with a dominant site at 28 kJ/mol, as determined by finite concentration IGC for *n*-pentane as molecular probe.

Keywords: Toner particles; Surface energy; Inverse gas chromatography; Automation; Adsorption

1. Introduction

Particle adherence studies by atomic force microscopy (AFM), using, for example, toner particles used in xerography, showed that the adhesion force depends on surface roughness and bulk mechanical properties of both the substrate and the particle, relative humidity, temperature, and the chemistry of the surfaces, which is reflected in surface energy characteristics [1,2]. One important factor in the explanation of adhesion phenomena as measured by AFM is the surface energy γ of the toner [1–3]. Determination of surface energy is essential for comparison between theoretical adhesion forces and AFM pull-off experiments. In this paper we discuss the surface energy characteristics of toner powder (for xerographic applications), studied by inverse gas chromatography (IGC).

The surface energy of native, irregularly shaped, toner particles is difficult to determine by contact

*Corresponding author. Present address: Materials Science and Technology of Polymers, Faculty of Chemical Technology and MESA+ Research Institute, University of Twente, PO Box 217, 7500 AE Enschede, Netherlands. Tel.: +31-53-489-2974; fax: +31-53-489-3823.

E-mail address: g.j.vancso@ct.utwente.nl (G.J. Vancso).

0021-9673/02/$ – see front matter
PII: S0021-9673(02)00374-6

angle measurements [4], even using a tablet made by compression in an infra-red mould [5]. The so-called Washburn method [6], in which the capillary rise of various liquids is monitored, also fails since many liquids are being absorbed into the bulk of the polymer matrix. In IGC the aforementioned experimental drawbacks are absent, or can be avoided [7].

IGC can probe the surface energy characteristics and other thermodynamic quantities of materials and can be performed over an extremely broad temperature range. Infinite dilution IGC (ID-IGC), i.e. experiments at zero surface coverage, provides the dispersive part γ_s^D of the total surface energy γ_s [8]. Another type of IGC experiment, finite concentration IGC (FC-IGC), provides the energy distribution $\chi(\epsilon)$ of ''surface active sites'', i.e. sites with adsorbing energies ϵ for gaseous probes [5,9,10]. To our knowledge, IGC has not been applied before to the study of the surface energy characteristics of toner powder.

The polyester-based toner powder investigated in this study [11] interacts with various surfaces in the xerographic process, such as the transport belt, the photoconductive plate, and the paper. AFM pull-off experiments, with toner particles attached to cantilevers, showed a broad distribution of pull-off forces. Moreover, multiple distributions of pull-off forces were found [12]. We expect this to be at least partially caused by the distribution of adsorption energy sites on the toner surface. Humidity-dependent pull-off experiments on toner particles resulted in increased adhesion forces above 70% relative humidity [12]. This suggests a hydrophilic toner surface, able to attract moisture and to bind to hydrophilic substrates through capillary forces. We verify these hypotheses in this study by means of FC-IGC, which enables surface energy distributions of functional groups at interfaces to be resolved. In order to investigate the contribution of the individual components in the toner particle (essentially a composite with a chemically and physically heterogeneous surface) to the total surface energy, three types of particles were studied: (a) commercial toner; (b) material (a) without carbon coating; and (c) polyester particles.

Bulk and surface properties of the stationary phase in IGC are derived from retention times or, more precisely, from net retention times [13]. The net retention time is the difference between two quantities of the same order of magnitude: the residence time of a probe interacting significantly with the stationary phase, and that of an inert probe, e.g. air or methane, depending on the detector used. Repeated measurements of both residence times are necessary in order to reduce the experimental error in the net retention time. This requires at least three injections of the same probe under the same experimental conditions.

The experimental conditions require accurate temperature control, to within 0.1 °C [7], and precise pressure detection of typically ±7 Pa [14]. In addition, an automatic sample injection unit is an essential element of an IGC set-up [15]. All this allows the collection of large numbers of chromatograms with high repeatability and, in combination with the use of automated data acquisition, data processing and measurement control, it speeds up the experiment considerably. Such automated IGCs may be useful for many applications, including combinatorial chemistry approaches to develop new materials [16]. Details on the benefits and on the acquisition structure of the automated set-up are included in Appendix A.

2. Theory

2.1. Adsorption and absorption determination

An IGC experiment probes the stationary phase with pure and known liquids or gases resulting primarily in the retention volume V_P. V_P is calculated from the first moment of the elution peak, t_P, multiplied by the carrier gas flow rate F. A marker, i.e. a ''probe'', which does not significantly interact with the stationary phase, is used to correct for the dead volume of the system. An additional factor J_3^2 is introduced to correct for gas compressibility. The so-called net retention volume (V_N), which is related to thermodynamic properties of the stationary phase, is calculated by using Eq. (1) [13]:

$$V_N = (t_P - t_M)FJ_3^2 = (V_P - V_M)FJ_3^2 \quad (1)$$

The sorption of a probe on the stationary phase

consists of two contributions: (a) the *ad*sorption on the surface and (b) the *ab*sorption into the bulk of the material. Depending on the permeability for the probe in the material, one of the two mechanisms dominates. These mechanisms can be distinguished in a Van 't Hoff plot, in which $\ln V_N$ is plotted as a function of $1/T$ (where T is the absolute temperature). These plots usually show two linear parts with a transition region in between [17]. In the linear part at low temperature (high $1/T$) adsorption takes place, and in the linear part at high temperature absorption dominates. Both mechanisms contribute to the total sorption in the transition region to the same extent.

2.2. Surface energy from infinite dilution IGC

2.2.1. Determination of γ_s^D

Surfaces can be characterized by γ_s. According to Fowkes [18], γ_s consists mainly of a London, or dispersive, part for interactions of non-specific nature (γ_s^D), and of a smaller specific, or polar, part (γ_s^P). These interactions are assumed to be independent and additive: $\gamma_s = \gamma_s^D + \gamma_s^P$. γ_s^D can be determined by injecting small amounts of *n*-alkanes as probes into the IGC column (the packing being the adsorbent of interest), and determining V_N for each sample. In principle, γ_s^P can be determined by injecting polar probes, but the interpretation of V_N in terms of γ_s^P is ambiguous, as will become clear below.

According to the frequently-applied method by Schultz et al. [19], γ_s^D can be determined by plotting $RT \ln V_N$ as a function of the quantity $a(\gamma_p^D)^{1/2}$, a so-called ''molecular descriptor'' [5]:

$$RT \ln V_N = 2N_{AV}(\gamma_s^D)^{1/2} a(\gamma_p^D)^{1/2} + k \quad (2)$$

where a is the area occupied by the probe molecule on the surface, and γ_p^D is the dispersive part of the surface tension of the liquid probe (interactions between *n*-alkanes and the surface are purely of a dispersive nature). N_{AV} is Avogadro's number, and k is a constant depending on the pressure and the spreading pressure of the adsorbate in a chosen reference state (this has been discussed in detail by Nardin and Papirer [8] and by Dorris and Gray [20]).

Determination of γ_s^D by Eq. (2) requires knowledge of the parameter a, which significantly depends on the models used [21]. The determination of the molecular area may be uncertain, particularly for non-spherical probes, e.g. *n*-alkanes [22]. Suggestions have been made in the literature to calculate the area from the molar mass and liquid density of the probe, assuming a hexagonal, closed-packing structure [23].

Eq. (2) is based on theoretical work of Dorris and Gray [20], who derived the method of plotting $RT \ln V_N$ as a function of the carbon number of the *n*-alkane probes. The slope of this plot gives γ_s^D according to:

$$\gamma_s^D = \frac{[RT \ln(V_{N(n+1)}/V_{N(n)})]^2}{4N_{AV}^2 a_{CH_2}^2 \gamma_{CH_2}} \quad (3)$$

in which the quantity between the square brackets is the slope of the plot just described, $V_{N(n)}$ and $V_{N(n+1)}$ are the net retention volumes of two injected *n*-alkanes with the consecutive carbon numbers n and $n+1$, a_{CH_2} is the area of a CH_2 group (0.06 nm^2) [20], and γ_{CH_2} is the surface energy of a solid surface consisting entirely of $-CH_2$ groups, such as polyethylene. The temperature dependence of γ_{CH_2} is often calculated according to $\gamma_{CH_2} = 35.6 + 0.058(20 - T)$ with T in °C and γ_{CH_2} in mJ/m^2 [19]. The average area occupied by the methylene group is derived by taking the value of 0.127 nm for the distance of separation between two carbon atoms and 0.47 nm for the average distance between the centers of the methylene groups in adjacent molecules [20]. Experimental evidence was given by Jacob and Berg from adsorption isotherm analysis [23].

The derivation of Eqs. (2) and (3), and consequently their limits of applicability, has been discussed by Nardin and Papirer [8]. In addition, these authors unified the approach of Eqs. (2) and (3) by the determination of γ_s^D from the slope K of a plot of $RT \ln V_N$ as a function of the saturated vapor pressure p_0 of the liquid probe:

$$RT \ln V_N = K \ln p_0 + \nu \quad (4)$$

where

$$K = \frac{3RT}{\chi(\gamma_0)^{1/2}} \cdot (\gamma_s^D)^{1/2} \quad (5)$$

The crucial molecular parameter in this approach is χ. It describes the number of ''interactions'' an atom or molecule can exchange with its neighbors, and depends on the number of nearest neighbors located around the atom or the molecule. For *n*-alkanes in a closed-packed structure χ is expected to be 3; the best experimental fit was 3.5 ± 0.01 [8]. The γ_0 in *K* is the surface energy of a non-polar solid which is homologous to the considered series of probes, e.g. polyethylene in the case of *n*-alkanes. The parameter ν is a constant that contains, apart from *K* and χ, another molecular parameter that could not be assessed unambiguously. Hence, Nardin and Papirer concluded that γ_s^D should be determined from Eq. (5) only.

In summary, all methods described above require accurate estimations of a specific molecular parameter, the area of the injected probe molecules, the surface energy and area of a CH_2 group, or the nearest neighbor parameter χ. All parameters are assumed to be independent of temperature and local topography, i.e. the interactions on the nanometer level are generally not considered. In addition it is required, from an experimental point of view, that the chromatographic peak in an ID-IGC experiment is symmetrical, i.e. not showing any tailing [13]. Furthermore, the elution times of the probes should be measured near zero surface coverage to prevent probe–probe interactions. Finally, the determination of the values of γ_s^D requires a flat surface, without any chemical or structural heterogeneity on the molecular scale [5].

2.2.2. Determination of specific components of the surface energy

The polar character of the stationary phase is studied by the employment of probes that can also interact through specific forces. If a polar probe is injected, an increase of V_N is expected. The ''extra part'' in the $RT \ln V_N$ value of a polar probe, above the ''apolar reference line'', is attributed to the polar component of the surface free energy, ΔG^P. The ''extra part'' significantly depends on the choice of the ''molecular descriptor'' on the *x*-axis [5,8,24]. Molecular descriptors include the three *x*-axis parameters mentioned in Section 2.2.1 (i.e. $a(\gamma_p^D)^{1/2}$, the carbon numbers and $\ln p_0$), but also the boiling point [25,26], the polarizability of the probe molecule [4], and the topology index χ_T [27,28] have been used.

2.3. Distribution of adsorption energy sites from FC-IGC

If a surface is heterogeneous with respect to energy, the ID-IGC results are mainly influenced by the highest-energy sites. In FC-IGC experiments, where significant volumes of the probe are injected [7], the sites with lower energy values also contribute to probe retention [5]. A special FC-IGC technique, the multiple-injection method, involves sequential injections with increasing amounts of probe [13,29]. Probing the higher- as well as the lower-energy sites reveals the chemical heterogeneity of the surface, which can be represented by the so-called energy-site distribution function. Such a function is a measure for heterogeneity and assists in tracking changes of the surface due to chemical and physical surface modifications. It can be used as a ''fingerprint'' to distinguish materials, e.g. minerals [9,10].

The following equations were used for calculation of the distribution $\chi(\epsilon)$ of adsorption energy sites ϵ [9,30–32].

$$\chi(\epsilon) = -\left(\frac{p}{RT}\right)^2 \cdot \left(\sum_{i=1}^{n} iB_i p^{i-1}\right) \cdot \exp\left(\sum_{i=0}^{n} B_i p^i\right) = -\left(\frac{p}{RT}\right)^2 \cdot \left(\sum_{i=1}^{n} iB_i p^{i-1}\right) \cdot V_N \quad (6)$$

and [10,33]:

$$p = \frac{RTn_1 H}{FJ_2^3 S_1} \quad (7)$$

In these formulae *i* and B_i are the polynomial exponents and fit parameters, respectively, of an exponential polynomial fit of V_N as a function of the partial pressure *p*. The probe is injected with a quantity n_1 (mol), *H* is the height of the elution peak (*V*), and S_1 reflects the surface area of the elution peak (V·s).

Eqs. (6) and (7), like Eqs. (2)–(5), are valid if adsorption takes place exclusively. Additionally, the family of distorted peaks must superimpose on the diffusion side [10], and the ideal gas law must hold for the gaseous probe.

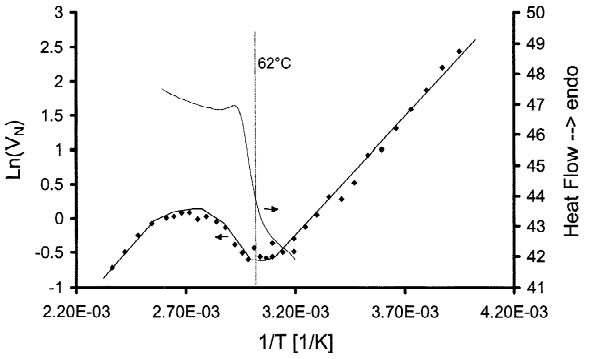

Fig. 1. Van 't Hoff plot of F10 toner material coated onto chromosorb, probed with *n*-pentane. The results are combined with the corresponding DSC micrograph.

3. Experimental

3.1. Equipment

A Shimadzu GC-14B equipped with a flame ionization detector and an AOC-20i auto injector was used. A CRG-15 cryogenic attachment was added in order to control the inlet of liquid nitrogen fed from a 50-l Apollo liquid nitrogen tank (Messer Griesheim, Krefeld, Germany). The pure polyester granules were first milled in order to increase the specific surface area, eliminating the need for extremely long columns. It should be noted that this procedure may slightly change the surface energy. It is known from the literature that, for example, milling and sieving of crystalline materials may introduce crystallographic facets having different surface energies [34]. Measurements below ambient conditions were established and a large temperature window of −80 to 400 °C could be covered. Liquid nitrogen was directly sprayed into the oven at a pressure of 1.5 bar. Additionally, a Brooks mass-flow controller 5850S together with a 0152 Brooks Microprocessor control and read-out unit were incorporated. The pressure was measured by a Druck PDCR911 pressure sensor ($0–4.0 \cdot 10^5$ Pa absolute), connected to a DPI 281 digital read-out unit. The injector and detector temperature was set to 100 °C. The SGE 0.5-μl autosampler syringe used enabled liquid and gas injection volumes of between 0.01 and 0.45 μl. Glass transition temperatures were independently measured by differential scanning calorimetry using a Perkin–Elmer DSC7 instrument.

The contact angle experiments were carried out by a conventional contact angle microscope (G10, Krüss, Hamburg, Germany). A drop of the polymer melt was formed at elevated temperature on a sample holder in a measurement chamber equipped with a heating element (Linkam, TMS93). During the measurement, pictures of the drop were taken at a fixed time interval using a CCD (Charge Coupling Device) camera. The drop contour was fitted by a DSA drop-shape analysis program (Krüss), which provided the values of the contact angle formed with the sample holder, the drop volume, and the surface tension. The contact angle was taken at both sides of the drop and the values were averaged.

3.2. Materials

Three types of toner particles were studied in this research: (a) commercially available ''F10'' polyester-based toner particles, (b) toner material (a) but deprived of their usual carbon coating, and (c) the pure polyester particles without any magnetic fillers and without the carbon coating. All toner particles were obtained from Océ-Technologies. The pure polyester was first milled (Pulverisette, Fritsch, Germany) with a grid of 0.5 mm in order to increase the specific surface area. Copper tubes of 1/4 in. O.D. were pre-cleaned with toluene, isopropanol and acetone (1 in. = 2.54 cm). The columns were cut to a length of ~1.2 m and filled with the different powders under investigation by using a mechanical vibrator and applying vacuum. Both ends of the columns were loosely plugged with quartz wool (Chrompack Nederland, Bergen op Zoom, Netherlands). The columns were conditioned under a stream of He for 2 days at 20 ml/min, below the T_g of the polyester. The T_g of the polyester was determined by IGC after coating it (5.0%, w/w) onto chromosorb G DMCS AW 60–80 mesh (Alltech, Breda, Netherlands). The polyester particles were dissolved in high-grade toluene, mixed with the chromosorb, and the toluene was slowly evaporated using a rotary evaporator. The carrier gas used was helium (purity 5.0, Praxair, Oevel, Belgium), and the flow rate was kept at 10.0 ml/min. The intrinsic gas hold-up, ''dead volume of the system'', was determined by

the injection of methane (purity 5.5, Praxair). The retention times were taken from the point of injection to the maximum peak height. All probes were high-grade *n*-alkanes obtained from Aldrich. The gas *n*-butane was obtained from Praxair. An average of five injections was recorded per probe.

4. Results and discussion

4.1. Surface energy of toner particles

4.1.1. Determination of the adsorption range

A temperature scan was performed in order to investigate the nature of the sorption mechanism as a function of temperature. The Van 't Hoff plot [35–37] using *n*-pentane as a probe is shown in Fig. 1. This plot shows a T_g of 62 °C for the polyester, which is the main constituent of the toner particles.

Bulk absorption usually dominates at experimental temperatures of 30–50 °C above the T_g of the polymeric stationary phase [38]. In our case this occurs at temperatures exceeding ~110 °C, where the Van 't Hoff plot has a linear part (at the lowest $1/T$ values). For the surface energy determination, an oven temperature below 30 °C was chosen. In this temperature range, where the Van 't Hoff plot has a linear part again (at the highest $1/T$ values), surface adsorption of the probe molecules largely exceeds probe absorption in the bulk in the contribution to V_N.

4.1.2. ID-IGC: apolar probes

A series of *n*-alkanes was injected at 30 °C. Small injected quantities were ensured by sampling from the gaseous phase of the liquid probes. The elution times of repeated injections were within 1%. The repeatability for the columns containing the pure toner particles was slightly less than observed with the column containing the polyester-coated chromosorb. This was probably due to less-than-ideal packing because of the irregular particle shape, or some bulk absorption of the probe into the polyester. In order to exclude absorption, experiments were also carried out at decreased temperature, typically 5 °C, thus further below the T_g of the polyester. The graphs from which γ_s^D values were obtained are shown in Fig. 2.

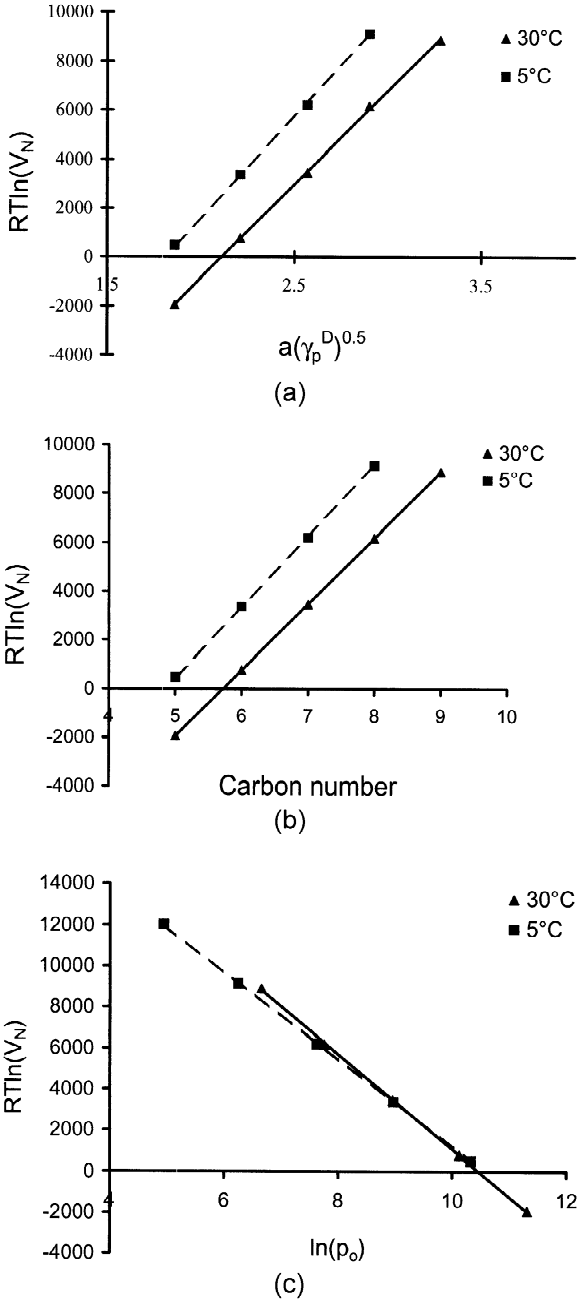

Fig. 2. The dispersive component of the surface energy of the toner polyester was determined according to three methods. $RT \ln V_N$ is plotted as a function of (a) the carbon number of the *n*-alkanes, (b) the area of the *n*-alkane multiplied by the square root of its surface tension (values were obtained from Ref. [19]; extrapolated values for *n*-butane and *n*-pentane were determined: 1.50 and 1.86 (nm^2 $(mJ)^{1/2}$ m^{-1}), respectively), and (c) the logarithm of the respective saturated vapor pressure (values obtained from Ref. [47] and $\chi = 3.5$ [8]).

Table 1
Summary of the determination of the dispersive component of the surface energy for different toner materials determined according to the methods presented in the theoretical section

Toner material	γ_s^D (mJ/m^2) (a) [20]		γ_s^D (mJ/m^2) (b) [19]		γ_s^D (mJ/m^2) (c) [8]	
	$T=5$ °C	$T=30$ °C	$T=5$ °C	$T=30$ °C	$T=5$ °C	$T=30$ °C
F10, pure polymer	43.6	40.1	47.3	40.5	42.7	40.3
F10, without carbon	–	44	–	44	–	44
F10	43	41	44	41	41	41

The surface energy at 5 °C, calculated [20] from Fig. 2a, was 43.6 mJ/m^2, whereas at 30 °C a value of 40.1 mJ/m^2 was found. According to the method by Schultz et al. [19], γ_s^D values of 47.3 and 40.5 mJ/m^2, respectively, were determined from Fig. 2b. Using the method based on the vapor pressure [8] of the *n*-alkane probe molecules and assuming $\chi=3.5$ [8], values of 42.7 and 40.3 mJ/m^2 were obtained, respectively. In conclusion, the three methods result in similar values at room temperature for γ_s^D, whereas at a lower temperature the Schultz method seems to overestimate this value. A decrease of the surface energy as a function of temperature is observed. In the literature this has been attributed to an entropic contribution to the surface free energy [39,40].

An overview of γ_s^D values of the various toner materials is given in Table 1.

Within experimental error, the γ_s^D part of the surface energy of the three types of toner particles is identical, and is largely associated with the polyester component. The other components of the toner composite have no detectable influence on this part of the surface energy. The statistical error in the elution times determined for the pure toner polyester was less than the value observed with the powder containing magnetic iron domains and carbon. This suggests that the surface of the toner powder is heterogeneous, which will be described in more detail below.

4.1.3. ID-IGC: polar probes

The polar component of the surface energy was investigated by probes exhibiting acid–base interactions with the stationary phase. The molecular structure of the polymer (a polyester [11]) suggests that strong interaction forces such as polar interactions and possibly hydrogen bonds may occur. As mentioned in the introduction, AFM pull-off experiments also suggest that such interactions are present. Sever-

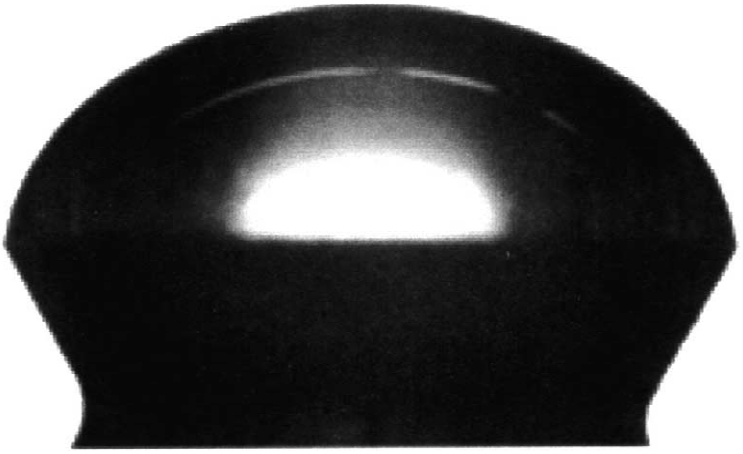

Fig. 3. Droplet of liquid polyester from F10 toner powder on the sample holder. From droplet analysis and quantification the surface tension is obtained.

al polar probes were injected in small amounts from the gaseous phase above the liquids. Tailing peaks were found for all probes, including methanol, ethanol, tetrahydrofuran, benzene, toluene, acetone, and diethylether. The elution peaks were at the detection limit of the detector and showed large retention volumes. For such peaks, quantitative interpretations are impossible [13]. From the strong specific interaction it can be qualitatively concluded that the toner surface has a hydrophilic nature, enabling polar interactions (and possibly hydrogen bonds).

4.1.4. Total surface energy determination by droplet analysis

Since we cannot compare the γ_s^D values by IGC to published results, a complementary determination of γ_s was carried out by contact angle measurements, using a special sample holder. In this method the polymeric material is heated above its T_g (and for semi-crystalline polymers well above their melting temperature), in order to degas it from residual solvent and air, and to ensure an equilibrated and smoothly-shaped droplet. From the shape of the liquid polymer surface the surface tension can be determined at the temperature of the melt [41–43]. Since the complete toner particle is intrinsically a composite material, a phase separation was observed between the polymer and the small solid pigment particles. The pure polymer, however, quickly formed a droplet with a smooth surface (Fig. 3).

Typically, ~18 mg of polymer was used for the size of the sample holder used in our equipment. After placing the sample in the measurement chamber, the temperature was raised to 100 °C with a heating rate of 10 °C/min. A sequence of pictures was acquired (one picture every 60 s) after the polymer was melted and equilibrated. The measurement always started with an isothermal heating period of 30 min after which the temperature was lowered with a cooling rate of 5 °C/min to the next measurement temperature. The experiments on the contact angle development of the polymer melt as a function of temperature were performed on the polyester. Fig. 4 shows a typical example of this experiment.

In Fig. 4 it can be seen that the contact angle decreases upon increasing the temperature, and that

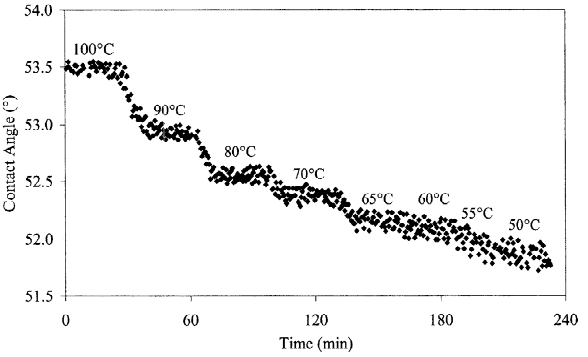

Fig. 4. Typical example of contact angle development as a function of temperature.

the properties of the melt change between 65 and 60 °C. Previous analysis by IGC and differential scanning calorimetry (DSC) (Section 4.1) has shown that the T_g of the material lies within this region, causing a non-equilibrated droplet.

The drop-shape analysis program uses a density of the drop equal to unity to calculate contact angle, drop volume, and surface tension. The only output parameter of the program that is dependent on density is the surface tension. The calculated volume of the drop, in combination with the mass of the sample, provides us with the value of the density at the temperature of measurement, thus also yielding the corrected value of the surface tension. Subsequently, the surface tension of the sample was plotted as a function of temperature (Fig. 5).

A decrease of the surface tension was observed, similar to the IGC experiments (Table 1). The values

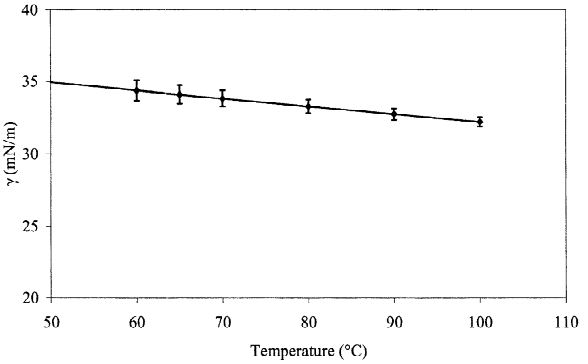

Fig. 5. Surface tension values at various temperatures of the polyester of the molten toner powder.

of the average surface tension are fitted with a linear curve: $\gamma = -0.054 \cdot T + 37.63$ (mJ/m^2). For amorphous polymers, it is assumed that no change in the slope occurs at T_g [41]. Subsequently, the surface tension values can be extrapolated to lower temperatures, below T_g. In this way, total surface energy values of 36.1 and 37.4 mJ/m^2 were determined for the polyester at 30 and 5 °C, respectively.

All γ_s^D values obtained by IGC were found to be higher than the values measured with this contact angle method. The contact angle method, however, should result in a higher value for γ_s, as $\gamma_s = \gamma_s^D + \gamma_s^P$. A possible explanation for the lower value found is that in the ID-IGC experiment the probes preferably bind to the high-energy adsorption sites at the surface of the particles [5,22,44]. The high-energy sites are predominantly probed, resulting in the higher surface energies observed compared to the overall measurement by contact angles [40,45]. This is in agreement with the statement at the end of Section 2.2.1 that the determination of the values of γ_s^D requires a flat surface, without any chemical or structural heterogeneity [5].

4.1.5. FC-IGC: energy site distribution

The surface energy site distribution of toner without carbon coating was probed with *n*-pentane. Stepwise increasing probe quantities were injected and the corresponding elution peaks are shown in Fig. 6.

The decreased interaction, i.e. smaller V_N, with increased probe concentration is indicative for surface heterogeneity [46]. The same argument as given in the previous section holds. If more probe molecules are available the more abundant sites with moderate surface energy will be probed, whereas at zero coverage the limited number of highly active sites is responsible for the large retention volume.

The distribution function χ as a function of the different energies is plotted in Fig. 7.

A broad distribution of surface energies for *n*-pentane as the molecular probe was measured with a dominant site at 28 kJ/mol. The distribution of sites present at the surface exhibiting different adsorption energy values is broad. This could explain why AFM pull-off experiments on toner showed multiple broad peaks [12].

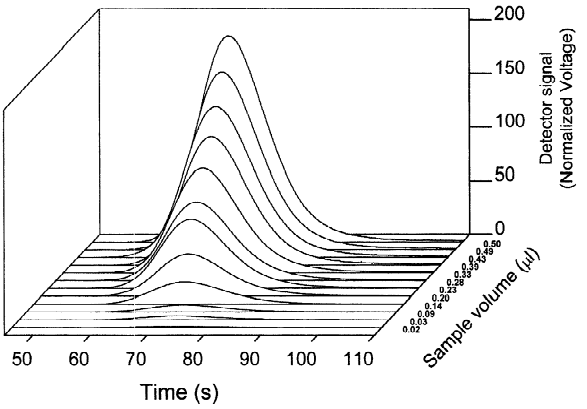

Fig. 6. Elution chromatograms obtained in a FC-IGC experiment with *n*-pentane on non-coated toner powder. The powder was applied directly in the IGC column without any chromosorb carrier. The peak development at numerous injected quantities is shown.

5. Conclusions

A custom-made automated inverse gas chromatography set-up was used to determine surface and bulk properties of toner particles. Data acquisition as well as the additional laborious calculations were carried out automatically, resulting in significantly increased system performance and throughput. A cryogenic attachment unit to the gas chromatograph enabled surface energy studies of materials exhibiting low glass transition temperatures.

Specifically, IGC was applied to study surface energy characteristics of polyester toner powders

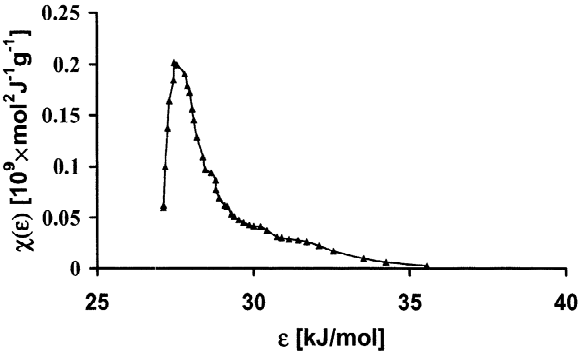

Fig. 7. Energy site distribution of F10 toner particles, without carbon coating, as the stationary phase. The probe *n*-pentane was injected at an oven temperature of 30 °C and the carrier gas flow rate was 8.0 ml/min.

below their T_g. The T_g was determined by IGC to be 62 °C, and confirmed by DSC. Values of γ_s^D were found to be between 40 and 45 mJ/m^2, for all three types of toner particles studied (toner particles, particles without the carbon coating, and polyester particles). This suggests that γ_S^D is determined by the polymeric component only. Several indications for surface heterogeneity were found: (i) the difference between γ_S^D determined by IGC and the unexpectedly lower total γ_s as determined by droplet analysis, (ii) the strong tailing of the peaks of the injected polar probes, (iii) the decrease of V_N with increasing *n*-pentane concentration, and finally (iv) the broad energy distribution function with a dominant site at 28 kJ/mol, as determined by finite concentration IGC for *n*-pentane as the molecular probe. In addition, the strong tailing behavior of the peaks of the injected polar probes suggests that the toner surfaces are strongly polar, and hydrophilic. These findings support previous observations in the pull-off experiments by atomic force microscopy.

Acknowledgements

The authors want to thank Océ-Technologies, Netherlands, for supplying materials and especially R.J.W. Lugtenberg for extensive discussions. M.A. Hempenius is acknowledged for his comments on the manuscript. G.J. Price and J.E. Guillet are gratefully acknowledged for inspiring discussions.

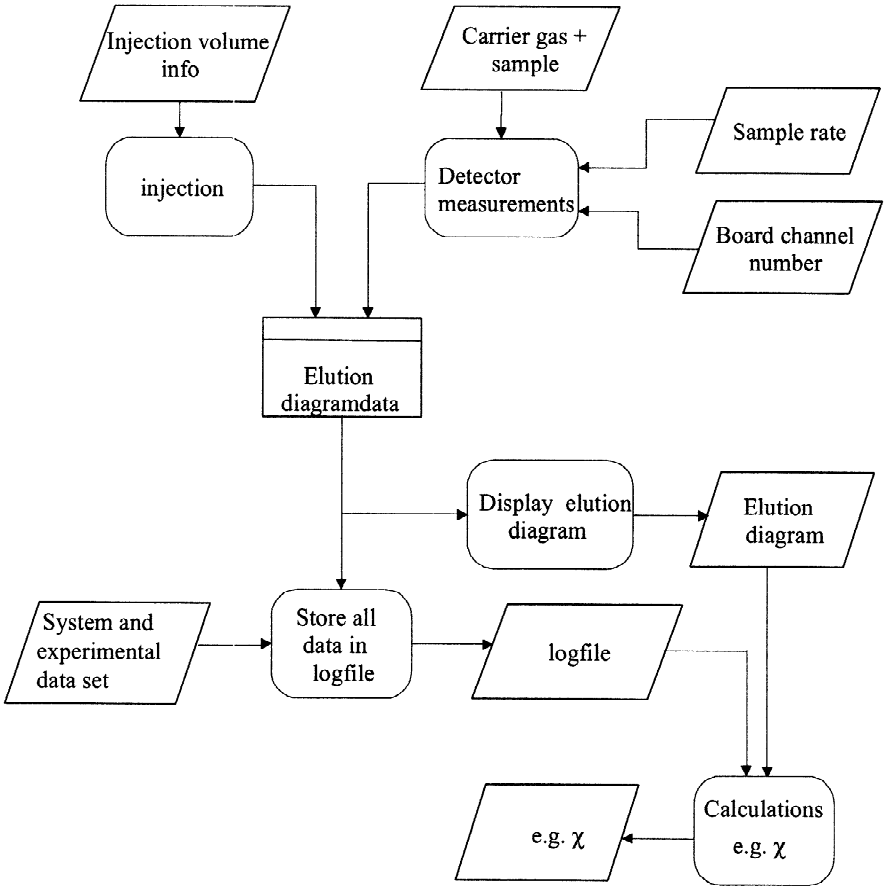

Fig. A.1. Data flow diagram of the automated IGC measurement.

Appendix A

A computer with custom-made software, developed in our laboratory, was used to run the experiments automatically and to process the data. A DAS-1601 data acquisition board by Keithley Metrabyte collected the electrical signals and converted them for processing on a standard Pentium PC. This 12-bit board proved to be adequate for a precise reading of the signal. The data were collected and processed in a program developed in our laboratory applying the 4th generation language TestPoint (Version 3.2b, Capital Equipment). Although sampling could be done at high rates, 11 Hz was enough to obtain good reproducibility combined with small data sets. The costs for the automation were limited to US$ ~2000 (excluding development labor costs). The data flow diagram summarizing the automation steps and necessary data units is given in Fig. A.1. The measurement itself can be performed by only a

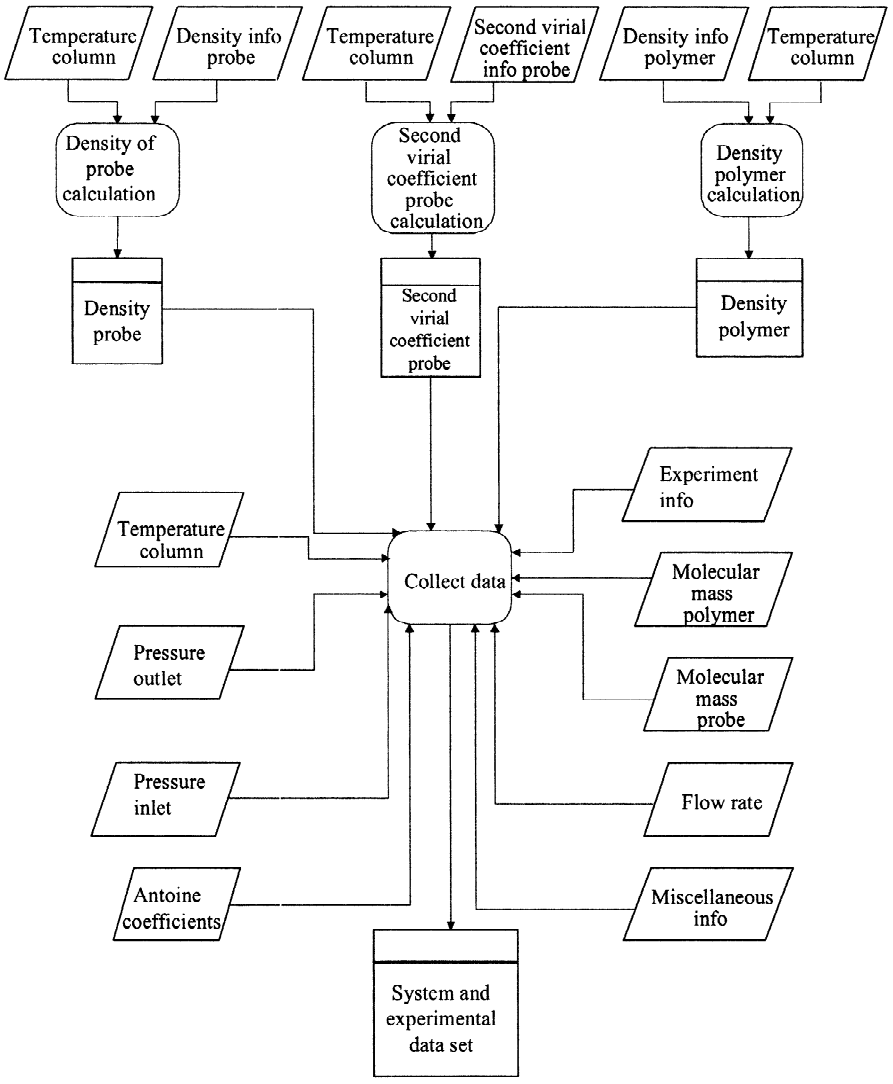

Fig. A.2. Detailed data flow diagram of necessary data input from the system, literature, and operator.

few parameters, recording the detector signal as a function of time after injecting a certain amount of probe in the carrier gas stream.

We chose the Flory–Huggins interaction parameter χ as a thermodynamic bulk quantity, which is frequently used in polymer engineering to predict miscibility and phase behavior. This parameter at infinite dilution of the probe is calculated essentially from the activity of the probe (Raoult's law) according to the equation (''1'' denotes the probe, ''2'' denotes the polymer) [48,49]:

$$\chi^{\infty} = \ln\left(\frac{273.15Rv_2}{V_g p_1^0 V_1}\right) - \left[1 - \frac{V_1}{(M_n)_2 v_2}\right] - \left(\frac{p_1^0}{RT}\right) \cdot (B_{11} - V_1) \quad \text{(A.1)}$$

with R representing the gas constant, $p_1^0(T)$ the saturated vapor pressure of the probe, $V_1(T)$ its molar volume, $v_2(T)$ the specific volume of the stationary phase, $(M_n)_2$ the molar mass of the stationary phase, and $B_{11}(T)$ the second virial coefficient of the probe in the mobile phase.

We decided to extend the automated data acquisition after our studies on the χ parameters of polymers. As can be concluded from Eq. (A.1) and the previously reported Eqs. (1)–(7), the surface, and especially polymer bulk parameters, require a large number of calculations. This applies particularly when varying the temperature for the determination of, for example, a Van 't Hoff plot, as almost every term in Eq. (1) and particularly Eq. (A.1) are temperature related. Therefore, these dependencies, e.g. the use of the Antoine equation for the vapor pressure, the Rackett equation for the molar volume and the relation for the virial coefficient, were integrated within the software of the automated set-up [47]. The compressibility correction factor, J_2^3 in Eq. (1) in the main text, varies also because of a change in inlet pressure, as a consequence of operating at different carrier gas flow rates or temperature. The data flow diagram (Fig. A.2) shows where the variables and experimental data are introduced in the data processing and calculations of thermodynamic polymer bulk variables such as the Flory-Huggins interaction parameter.

The automated system produces the end results significantly faster, by up to five times, than the non-automated version. One of the most important reasons for this is that the peak analysis can be performed on-line and that the data for numerical calculations to obtain the desired materials properties are generated in situ. The 4th generation computer language Testpoint allowed us to build quickly and efficiently a user-friendly graphical interface with corresponding storage, analysis, and calculations. In conclusion, because of the fact that the data acquisition as well as the additional laborious calculations are performed automatically, system performance and throughput are significantly increased. The improved throughput allows quick determination of repeatability resulting in reduced standard deviations of the retention times.

References

[1] K.L. Johnson, K. Kendall, A.D. Roberts, Proc. R. Soc. London, Ser. A 324 (1971) 301.
[2] D. Tabor, J. Colloid Interf. Sci. 58 (1977) 2.
[3] J.N. Israelachvili, in: A.T. Hubbard (Ed.), Handbook Surface Imaging Visualization, CRC Press, Boca Raton, FL, 1995, p. 793.
[4] J.B. Donnet, H. Balard, Chromatographia 31 (1991) 434.
[5] E. Papirer, E. Brendle, F. Ozil, H. Balard, Carbon 37 (1999) 1265.
[6] E.W. Washburn, Phys. Rev. 17 (1921) 273.
[7] G.J. Price, J.E. Guillet, J. Macromol. Sci. A23 (1986) 1487.
[8] M. Nardin, E. Papirer, J. Colloid Interf. Sci. 137 (1990) 534.
[9] M.-J. Wang, S. Wolff, J.-B. Donnet, Kautsch. Gummi. Kunstst. 45 (1992) 11.
[10] S. Rebouillat, J.B. Donnet, H. Guo, T.K. Wang, J. Appl. Polym. Sci. 67 (1998) 487.
[11] M.L.M. Pennings, R.A.M. Venderbosch, W.H.G. Albrink, G.J. Crommentuyn, US Patent 5 296 327, 1992.
[12] L.H.G.J. Segeren, F.G. Karssenberg, J.P. Pickering, J.W.A. van den Berg, G.J. Vancso, in: K.L. Mittal (Ed.), Particles on Surfaces 7: Detection, Adhesion and Removal, VSP, Utrecht (in press).
[13] J.R. Conder, C.L. Young, Physicochemical Measurements by Chromatography, Wiley, New York, 1979.
[14] G. Dipaola-Baranyi, J.E. Guillet, Macromolecules 11 (1978) 228.
[15] S. Panda, Q. Bu, K.S. Yun, J.F. Parcher, J. Chromatogr. A 715 (1995) 279.
[16] C.J. Hawker, E. Harth, D. Benoit, T. Bosman, World Polymer Congress IUPAC Macro 2000, 38th Macromolecular IUPAC Symposium, Warsaw, 2000, p. 12.
[17] A. Lavoie, J.E. Guillet, Macromolecules 2 (1969) 443.
[18] F.M. Fowkes, Ind. Eng. Chem. 56 (1964) 40.
[19] J. Schultz, L. Lavielle, C. Martin, J. Adhesion 23 (1987) 45.
[20] G.M. Dorris, D.G. Gray, J. Colloid Interf. Sci. 77 (1980) 353.

[21] T. Hamieh, M. Rezzaki, J. Schultz, Colloids Surfaces A 189 (2001) 279.
[22] P. Mukhopadhyay, H.P. Schreiber, Colloids Surfaces A 100 (1995) 47.
[23] P.N. Jacob, J.C. Berg, Langmuir 10 (1994) 3086.
[24] M.C. Gutierrez, J. Rubio, F. Rubio, J.L. Oteo, J. Chromatogr. A 845 (1999) 53.
[25] D.T. Sawyer, D.J. Brookman, Anal. Chem. 40 (1968) 1847.
[26] D.J. Brookman, D.T. Sawyer, Anal. Chem. 40 (1968) 106.
[27] E. Brendlé, E. Papirer, J. Colloid Interf. Sci. 194 (1997) 207.
[28] E. Brendlé, E. Papirer, J. Colloid Interf. Sci. 194 (1997) 217.
[29] J.R. Conder, J. High Resolut. Chromatogr. Chromatogr. Commun. 5 (1982) 341.
[30] W. Rudzinski, A. Waksmundzki, R. Leboda, Z. Suprynowicz, M. Lason, J. Chromatogr. 92 (1974) 25.
[31] W.T. Cooper, J.M. Hayes, J. Chromatogr. 314 (1984) 111.
[32] M.-J. Wang, S. Wolff, Rubber Chem. Technol. 65 (1992) 890.
[33] R.-Y. Qin, J.B. Donnet, Carbon 32 (1994) 165.
[34] H.E. Newell, G. Buckton, D.A. Butler, F. Thielmann, D.R. Williams, Pharm. Res. 18 (2001) 662.
[35] J.-M. Braun, J.E. Guillet, Macromolecules 8 (1975) 882.
[36] S. Panda, Q. Bu, B. Huang, R.R. Edwards, Q. Liao, K.S. Yun, J.F. Parcher, Anal. Chem. 69 (1997) 2485.
[37] J.F. Parcher, R.R. Edwards, K.S. Yun, Anal. Chem. 69 (1997) 229A.
[38] Ö. Cankurtaran, F. Yilmaz, Polymer Int. 41 (1996) 307.
[39] W. Shen, I.H. Parker, Y.J. Sheng, J. Adh. Sci. Technol. 12 (1998) 161.
[40] B. Riedl, P.D. Kamdem, J. Adh. Sci. Technol. 6 (1992) 1053.
[41] B.W. Cherry, Polymer Surfaces, Cambridge University Press, Cambridge, 1981.
[42] D.W. van Krevelen, Properties of Polymers, Elsevier, Amsterdam, 1990.
[43] S. Wu, Polymer Interface and Adhesion, Marcel Dekker, New York, 1982.
[44] H. Balard, O. Aouadj, E. Papirer, Langmuir 13 (1997) 1251.
[45] N.M. Ahfat, G. Buckton, R. Burrows, M.D. Ticehurst, Eur. J. Pharm. Sci. 9 (2000) 271.
[46] A. Asten, N. van Veenendaal, S. Koster, J. Chromatogr. A 888 (2000) 175.
[47] D.R. Lide, H.V. Kehiaian, CRC Handbook of Thermo-Physical and Thermo-Chemical Data, CRC Press, Boca Raton, FL, 1994.
[48] A. Smidsrød, J.E. Guillet, Macromolecules 2 (1969) 272.
[49] Z. Tan, G.J. Vancso, Macromolecules 30 (1997) 4665.